Adsorption of lead ion from aqueous solution unto cellulose nanocrystal from cassava peel

IOP Conf. Series: Journal of Physics: Conf. Series **1299** (2019) 012122 doi:10.1088/1742-6596/1299/1/012122

Adsorption of lead ion from aqueous solution unto cellulose nanocrystal from cassava peel

Chioma Vivian Abiaziem[1,2*], Akan Bassey Williams[1], Adedayo Ibijoke Inegbenebor[1], Chionyedua Theresa Onwordi[3,4], Cyril Osereme Ehi-Eromosele[1], Leslie Felicia Petrik[3]

[1]Department of Chemistry, Covenant University, Km 10, Canaan Land, Ota, P.M.B 1023, Ota, Ogun State, Nigeria

[2]Science Laboratory Technology Department, The Federal Polytechnic Ilaro, P.M.B 50, Ilaro, Ogun State, Nigeria

[3]Department of Chemistry, Environmental and Nano Sciences Group, University of the Western Cape, Bellville, Cape Town, 7535, South Africa

[4]Department of Chemistry, Lagos State University, Ojo, LASU P.O.Box 0001, Ojo, Lagos State, Nigeria

*Corresponding author E-mail address: vyvycox@yahoo.com

Abstract. Acid hydrolysis was used for the synthesis of cellulose nanocrystal (CNC) from cassava peel (CP). The process was carried out at 45^0C for 45 min using 64% concentrated sulphuric acid, Pb^{2+} was removed from aqueous solution using the synthesized CNC adsorbent. Cassava peel cellulose nanocrystal (CPCNC) was characterised using FT-IR and X-Ray diffraction techniques. The different operational factors were examined to enhance the conditions for optimum adsorption of Pb^{2+}. The equilibrium adsorption figures fitted well into both the Freundlich and Langmuir isotherm models, indicating that adsorption was due to the formation of a monolayer adsorption unto a homogenous surface and showed a good relationship between the Pb^{2+} and the CPCNC. The separation factor, RL, which is a dimensionless constant ranged between 0.02 and 0.248 and indicated that the adsorption was feasible and favourable. The optimum adsorption capacity was 6.4 mg Pb^{2+}/g CNC at 25^oC and pH 6. This study revealed that this novel nanomaterial has an unlimited prospect for effective removal of lead ion from aqueous solution.

Keywords: Adsorption, Pb^{2+}, cellulose nanocrystal, cassava peel, aqueous solution, adsorption isotherm.

1. Introduction

There has been an increasing unavailability of clean, safe and potable source of water in all parts of the biosphere in the last few years. Research has shown that over 700 million people have no access to potable, clean water or satisfactory sanitation [1]. Environmental pollution, especially water pollution, stands as a risk to the global water supply. Examples of these environmental pollutants are heavy metals such as mercury, lead, chromium, arsenic, cadmium, copper, among others. These metals lead to environmental pollution from a number of origins, such as effluents from industries, discharge of metal ions from the soils into lakes and rivers by acid rain, weathering of sedimentary rocks etc. At low levels/concentrations, they pose serious threat to human health and the environment [1][2].

In understanding the growing bid for "green" and sustainable technologies for water treatment, natural polymeric materials have been extensively examined as ways of substituting synthetic and inorganic wastewater treatment with natural polymers[3][4]. In the recent years, agro-wastes such as sugarcane bagasse, sweet potatoes residue, palm kernel shell, coconut shell, bamboo, rice straw, walnut husks, rice husks etc. which are low-cost, available and economically viable have been reported to be prepared into cellulose nanocrystals and used as adsorbents for the treatment of wastewaters [5][6][7]. Cellulose nanocrystal, which is a grouping of biosorption, nano sizes and cellulosic nature, has a remarkable prospect for a novel and green part to resolve the present heavy metal pollution problems due to its unique properties such as high surface area, reduced toxicity, low cost, low density, biodegradability and biocompatibility. [8][9][10]. This is unlike the conventional methods such as ion exchange, chemical precipitation, solvent extraction, electrodialysis which are non-economical and have several limitations including generation of toxic sludge, incomplete removal of metal ions, high energy requirement etc[5].

Cassava (Manihot esculent Crantz) commonly known as Manioc is a perennial woody shrub grown annually. Cassava is largely produced in Brazil, Thailand, Nigeria, Zaire and Indonesia. They represent about 5-15% of the root. They comprise high quantities of cyanogenic glycosides and higher protein constituents compared to other tuber parts and are used as feeds for ruminants, livestock and fishes [11][12].

In this research, the potential of cellulose nanocrystal prepared from cassava peel for the removal of Pb^{2+} from aqueous solution was investigated. The equilibrium adsorption data of Pb^{2+} concentration unto CPCNC was studied with adsorption isotherm; Langmuir and Freundlich models.

2. Materials and Methods

2.1. Materials

The Cassava peels used in this study were collected from different cassava processing plants at Ilaro and Owode areas in Ogun State, Nigeria. Chemicals used were toluene, ethanol, sodium hydroxide, sodium chlorite, acetic acid and sulphuric acid. All the reagents were of analytical grade and purchased from Sigma Aldrich and Merck South Africa. Ultra-pure water was used for dialysis.

2.2 Isolation of Chemically Purified Cellulose

The sample was air-dried for several days, milled and sieved with a 30 mesh sieve. The purified cellulose (CPC) from cassava peel was isolated with minor modifications as

described by [13][14][15][16]. The cassava peel (30 g) was extracted with toluene to ethanol mixture of 2:1v/v for 6 h and then oven-dried at 60°C for 16 h. The dewaxed sample was soaked in 50 g/L of 5% sodium hydroxide solution to sample at 25^{o}C for 24 h followed by heating at 90^{o}C for 2 h to remove hemicellulose and silica. This was washed with plentiful amount of distilled water until neutral pH was achieved, followed by drying at 50^{o}C for 16 h. The residual alkaline treated sample was then delignified using 2.5 % w/v of acidified sodium chlorite with fibre to solution part of 1:20 for 4 h at 100^{o}C.The delignified cellulose was, thereafter, washed with water, oven-dried at 50^{o}C for 16 h. Finally, the product (chemically purified cellulose) was collected.

2.3 Synthesis of Cellulose Nanocrystals

Chemically purified cellulose (α-cellulose) produced from peel of cassava was synthesised into cellulose nanocrystal by acid-hydrolysis, according to the method adopted [17][14][16][13] with little modifications. The cellulose isolated from cassava peel was hydrolysed with 64 wt.% sulphuric acid at a 10 mL/g at a temperature of 45^{o}C for 45 min with vigorous stirring. Hydrolysis reaction was quenched by diluting with 10-times chilled water. The resultant cellulose nanocrystal gel was centrifuged at 45000 rpm for 30 min to concentrate the cellulose nanocrystal and to eliminate extra aqueous acid, the filtrate was then decanted. The resultant precipitate was dialysed with cellulose dialysis tube (Sigma –Aldrich, South Africa) against ultra-pure water until attaining neutral pH (pH 6-7). The suspension was sonicated at an amplitude of 40% in an ice bath to disrupt solid aggregates and avoid overheating. The resultant CNC suspension was freeze-dried (–47^{o}C, 0.2 mbar). The dried sample was preserved in a sealed container for characterisation.

2.4. Characterisation

2.4.1. Fourier Transform Infra-Red Spectroscopy (FT-IR)

FT-IR was used to determine the functional groups of the molecules. The PerkinElmer spectrum 400 FT-IR spectrometer was programmed at a resolution of 2.0 cm^{-1} to scan 60 times.

2.4.2. X-Ray Diffraction (XRD) Spectroscopy

X-ray diffraction was carried out using Philips X-pert MPD X-ray diffractometer with Cu-K radiation operating at 40 kV and 40 Ma, to identify the crystallinity nature of a material. The sample was scanned over a range of 5^{o} to 70^{o} 2θ with the count step size programmed at 0.5 seconds per step/0.05 step size. The maximum intensity of the principle peak of 200 (I_{002}, 2θ= 22.9°) was calculated from crystallinity index (CI) and the intensity of diffraction of 110 peaks (I_{am}, 2θ=16°) using the Seagal method [18] [19].

$$CI(\%) = \frac{I_{002} - I_{am}}{I_{002}} \times 100 \quad (1)$$

I_{002} represent crystalline material, whereas Iam represent the amorphous material.

2.5. Adsorption of Lead Ion

The adsorption experiment of Pb^{2+} unto cassava peel nanocrystal (CPCNC) was carried out in batch and in duplicate on a shaker at 200 rpm at 25^{o}C using 150 mL shaker flasks. The effects of pH, adsorbent dosage, initial concentration, contact time and temperature using the synthesised cellulose nanocrystals was studied on the adsorption process. The pH was attuned at a maximum pH of 7 to avoid formation of insoluble lead hydroxide. The Pb^{2+} was analysed using ICP-OES Varian Radial, Varian 710-ES technique, the adsorption capacity (qe) and percentage removal were calculated as described in equations 2 and 3b respectively.

$$q_e = \frac{(C_O - C_e)V}{W} \quad (2)$$

$$R = \frac{C_o - Ce}{C_o} \quad (3a)$$

$$R\% = \frac{C_o - Ce}{C_o} \text{ X } 100 \quad (3b)$$

Where, q_e is the equilibrium capacity one gramme of the adsorbent (mg/g), C_o is the concentration of the Pb^{2+} (mg/L), Ce is equilibrium concentration of Pb^{2+} (mg/L), W is the dry weight of the nano-adsorbent (g), V = solution volume (L), R is heavy metal removed/adsorbed, R% is percentage of heavy metal removed/adsorbed.

2.5.1. Langmuir Isotherm

In Langmuir model all adsorbed ions meets the surface layer of the adsorbent with a determinate number of similar sites. There is no drifting of adsorbate in the plane of the surface and there is regular pattern vigour of adsorption onto the surface [20]. The straight pattern of Langmuir shows:

$$\frac{1}{q_e} = + \frac{1}{Q_m b C_e} \quad (4)$$

Where,

q_e = Quantity of lead ion adsorbed per gramme of the adsorbent (mg/L)
Q_m = Maximum cover volume of the adsorbent (mg/g)
b = Langmuir isotherm constant (L mg^{-1})
C_e = Equilibrium concentration of the adsorbate (mg/L)

The values of q_e and b were evaluated from the slope and intercept of the Langmuir plot of the $\frac{1}{q_e}$ against $\frac{1}{C_e}$. The Langmuir isotherm was stated as a constant (R_L), an equilibrium parameter.

$$R_L = \frac{1}{1 + (1 + bC_o)} \quad (5)$$

Where, C_o = initial concentration of the adsorbate (mg/L)

2.5.2. Freundlich Isotherm

This explains the features of a mixed surface and was ascertained by using the computation below [21]:

$$q_e = K_f C_e^{\frac{1}{n}} \quad (6)$$

Where,

q_e = Amount of the heavy metal that had been adsorbed at equilibrium (mg/g)

K_f = Freundlich isotherm constant (mg/g)

n = Adsorption intensity

C_e = Equilibrium concentration of the adsorbate (mg/L)

$\frac{1}{n}$ = the function of the strength of the adsorption

The linear equation of the equ.6 will be given as:

$$\ln q_e = \ln K_f + \frac{1}{n} \ln Ce \quad (7)$$

3. Results and Discussion

3.1. FT-IR Analysis

The functional groups present in the cassava peel samples were examined using the FT-IR technique. (CP). Figure 1 shows the FTIR spectra of CP, CPCPC and CPCNC, the characteristic intense peaks that occur at 3333 cm^{-1} and 3272 cm^{-1} for CNC, CPC and CP respectively, that is associated to the O-H groups linked with water in the fibre. CNC, CPC and CP show a stretching frequency at 2892 cm^{-1}, 2906 cm^{-1} and 2920 cm^{-1} respectively and are ascribed to the C-H symmetric vibrations and 1640 cm^{-1} and 1625 cm^{-1} emanating from the absorbed water. Peaks at 1320 and 1427 cm^{-1} of SP, SPCPC and SPCNC are attributed to the bending of CH and CH_2 which indicates polysaccharides while 1163 and 1149 cm^{-1} of CNC, CPC and CP are due to (C=O=C) asymmetric vibrations [17][22]. The characteristic bands of cellulose are obvious at frequencies 1035 and 1007 cm^{-1} of CNC, CPC and CP respectively, conforming to C=O=C pyranose ring of all the spectra [23][24]. The peak at 765 cm^{-1} in the raw sample disappeared in the treated sample indicating the removal of silica. The peaks between 1398 and 1177 cm^{-1} of the nanocellulose is indicative of sulphonates in nanocellulose sample [25].

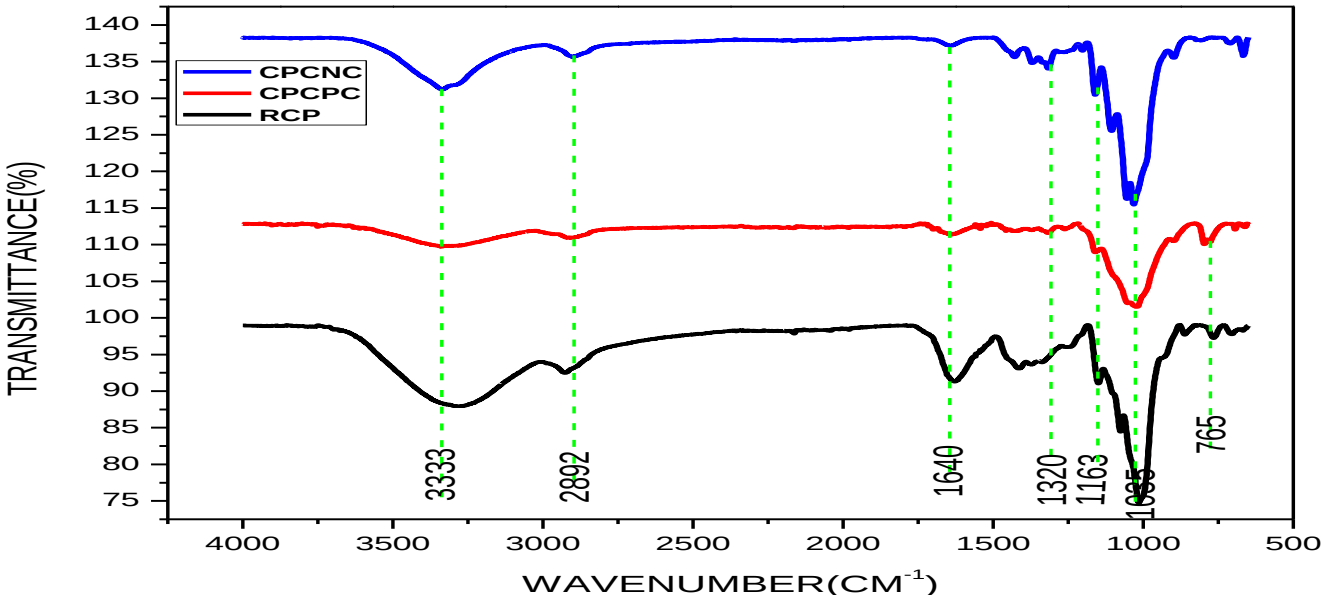

Figure 1: FT-IR spectra of raw cassava peel (RSP), cellulose fibre (SPCPC), cellulose nanocrystal (CPCNC)

3.2. X-Ray Diffraction

The crystalline structure and phase purity of cassava peel (CP, CPCPC and CPCNC) were analysed by X-ray diffraction analysis as display in Figure 2. The distinctive peaks for the raw sample absorbed at 2θ= 17.65°, 15.02° and 34.19° which correspond to 110 and 400 lattice planes of cellulose structure respectively, indicating the presence of lignin and hemicellulose[24][13]. Also, the peaks at 2θ= 12.39° and 22.91° respectively for CPCPC, which correspond to lattice planes of 110 and 200, indicating cellulose and the disappearance of the peak at 400 indicates the partial removal of amorphous region [26][27]. The decreased intense peak at 2θ=12.0° of the CPCNC indicates the complete elimination of the amorphous domain. The broad peak of the CPCNC indicates the disruption of the non-crystalline domain which results in increased degree of crystallinity, leading to broader surface area and higher specific strength of the CPCNC. The X-ray diffractograms show a main intensity peak which is situated at 2θ value of about 22.71° indicating the crystallinity configuration of cellulose, while the less intensity peak at a 2θ value of about 12° -14° is considered as non-crystalline domain [14]. The crystallinity index of CP, CPCPC and CPCNC was calculated to be 60.70%, 91.72%, and 99.86%, similar to the data obtained by [28]. The crystallinity index increased progressively from the raw to the CNC, showing a similar trend to the results earlier reported [29] [14]. The high crystallinity index indicates the presence of high CPCNC crystallites. The progressive increase of the crystallinity index from raw to CNC implies the removal of lignin, hemicellulose and extractives [30][31][32]. The XRD crystallite particle size for cassava peel showed a trend from untreated to CNC to be 25.39, 24.10 and 5.56 nm respectively.

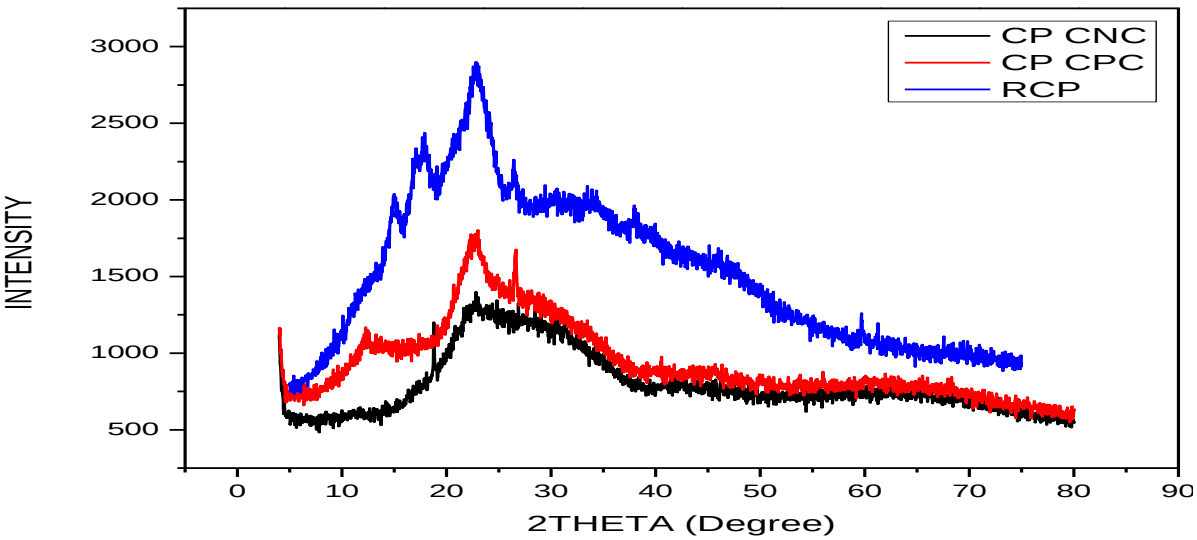

Figure 2: X-ray diffraction of raw cassava peel (RCP), cellulose (CPCPC), cellulose nanocrystal (CPCNC)

3.3. Adsorption Analysis of Lead Ion onto CPCNC

3.3.1. Effect of Solution pH

Figure 3a presents the amount of Pb^{2+} adsorbed and the percentage Pb^{2+} removed on CPCNC at various pH. The data revealed that the adsorption bulk was high as the pH enhanced from 2 to 6, and then decreased after pH 6. The results revealed that CPCNC adsorbents was reliant on the pH of the lead ion aqueous solution. At the acidic medium (low pH), the adsorbent active sites were scanty for Pb^{2+}, because of the presence of protons on the active sites possessing high hydrogen ion concentration [33]. Conversely, as the concentration of hydrogen ion declined the degree of proton on the functional group surface decreased due to electrostatic attraction, which enhanced the adsorption capacity of the adsorbent. The adsorption characteristic was observed to be dependent on pH, and the optimum adsorption was seen to be near neutrality, pH 6; the adsorption was considerably lesser in acidic pH conditions, as hydrogen ion competed with Pb^{2+} for the sulphate functional groups on the cellulose nanocrystal superficial [34]. Moreso, when there is an increase in pH, the concentration of hydrogen ion reduces and the amount of proton on the surface functional groups reduces, thus enhancing the adsorption bulk of the CPCNC adsorbent. The optimum adsorption capacity for Pb^{2+} (6.4 mg/g or 86.02%) was attained at pH 6, similar to the result reported by [35]. The adsorption capacity reduced at pH 7 to 1.92 mg/g or 51.06%.

3.3.2. Effect of Initial Concentration of Lead Ion

Figure 3b presents the amount of Pb^{2+} adsorbed and the percentage of Pb^{2+} removed on CPCNC at various initial concentrations. The result revealed that the capacity of Pb^{2+} adsorbed increased as the initial concentration enhanced from 5 ppm to 30 ppm. The amount of Pb^{2+} adsorbed on the CPCNC decreased from 40 ppm. This could be attributed to the realisation that at low concentration, there are additional adsorption sites present for the uptake of Pb^{2+} and at higher concentration there are less adsorption sites [33]. However, the

percentage removal of Pb^{2+} initially increased with no significant difference from 5-20 ppm and gradually decreased significantly with increase in the initial Pb^{2+} concentration. As the concentration of Pb^{2+} increased the adsorption sites of the adsorbent became completely occupied because of the presence of more Pb^{2+} concentration and could no longer adsorb Pb^{2+} from the solution hence, the adsorption capacity reduced.

3.3.3. Effect of Contact Time

A fast contact time to attain optimisation indicates a quick transferal of the metal ions from the solution to the heterogeneity of the adsorbent (CPCNC). The quantity of Pb^{2+} adsorbed and percentage of Pb^{2+} removed are presented in Figure 3c. The level of removal was somewhat steady from contact time between 15 to180 min, after 180 min the quantity of Pb^{2+} adsorbed decreased, indicating that the adsorbent site was saturated with Pb^{2+} at a longer time; this end result is similar to that stated by [36]. The optimum time was fast at 30 min (14.43 mg/g and 99.93%) for quantity of Pb^{2+} adsorbed and percentage of Pb^{2+} removed respectively.

3.3.4. Effect of Temperature

Figure 3d presents the amount of Pb^{2+} adsorbed on CPCNC at different temperatures. The result shows that as the temperature increased both the percentage removal and the amount of Pb^{2+} adsorbed decreased. This could be attributed to the reduction in activity of the surface, signifying that adsorption amid Pb^{2+} and the adsorbent (CPCNC) exhibited an exothermic reaction [37]. The decrease in removal of Pb^{2+} as temperature increased could be that at high temperature the active sites of the adsorbent decreased while the border cover of the adsorbent with temperature increased in thickness, hence the resistance of the adsorbate in the border layer increased [36]. The maximum percentage removal and amount of Pb^{2+} adsorbed occurred at 25^{o}C.

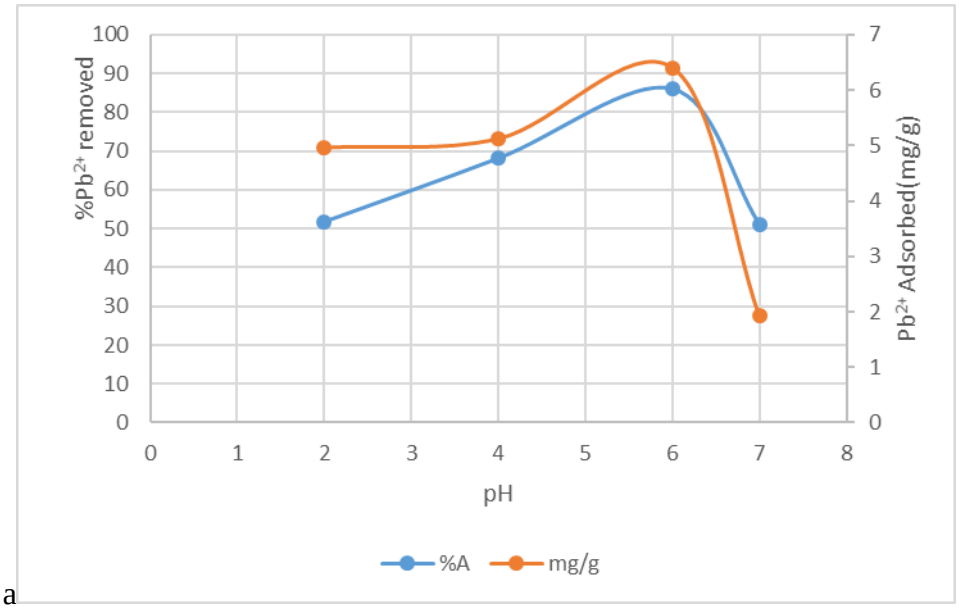

a

b

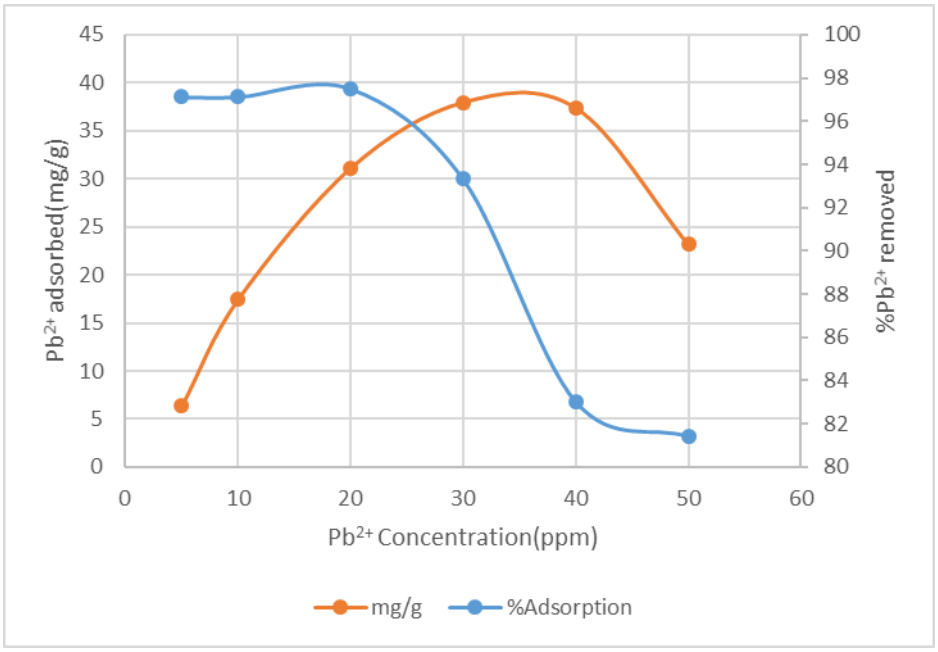
45
40
35
30
25
20
15
10
5
0
100
98
96
94
92
90
88
86
84
82
80
0
10
20
30
40
50
60
Pb2+ adsorbed(mg/g)
%Pb2+ removed
Pb2+ Concentration(ppm)
mg/g
%Adsorption

c

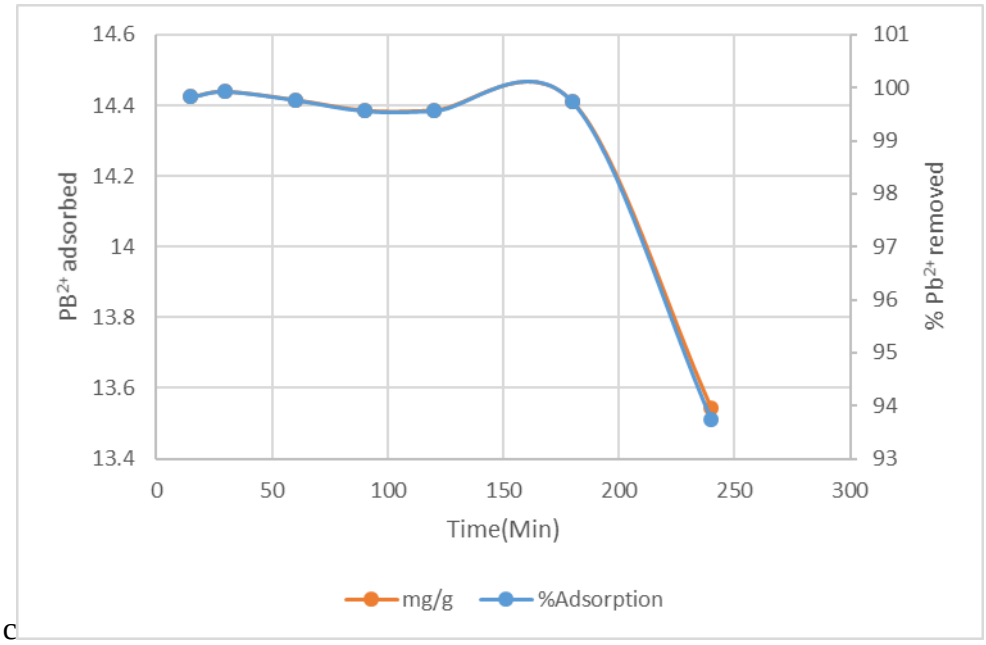
14.6
14.4
14.2
14
13.8
13.6
13.4
101
100
99
98
97
96
95
94
93
0
50
100
150
200
250
300
PB2+ adsorbed
% Pb2+ removed
Time(Min)
mg/g
%Adsorption

d 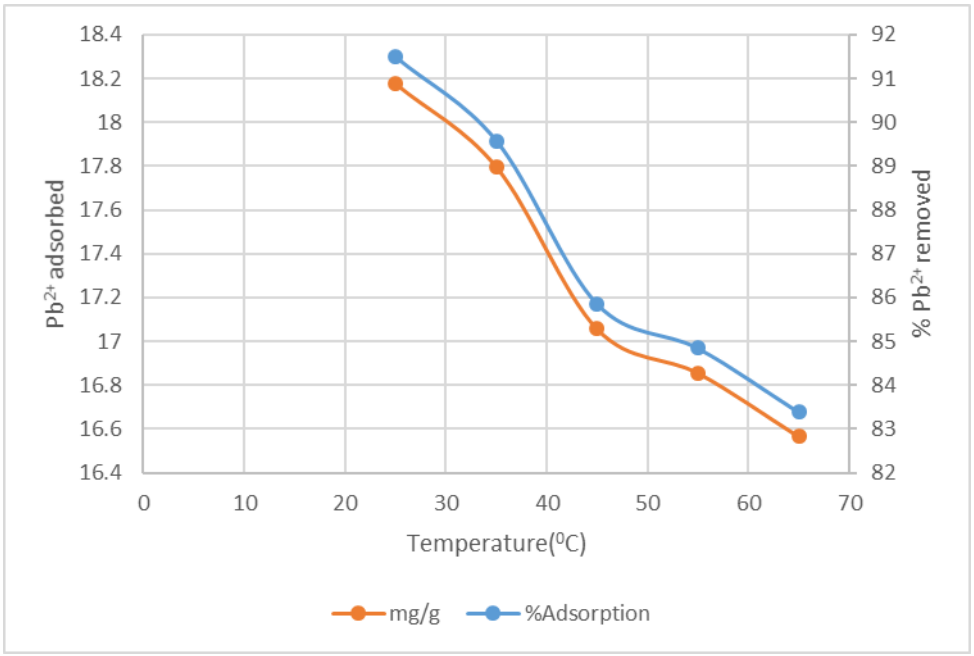

Figure 3: Effect of (a) pH (b) initial Pb^{2+} concentration (c) contact time and (d) temperature on the adsorption of Pb^{2+} unto CPCNC

3.4. Adsorption Isotherms

3.4.1. Langmuir and Freundlich isotherms for adsorption of Lead ion onto CPCNC

Adsorption isotherms were determined using Langmuir and Freundlich models, following equations 4 and 7 respectively. Adsorption isotherms interpret interaction between adsorbates and adsorbents. The optimum adsorption capacity can be achieved from the isotherms. This study covers Langmuir and Freundlich isotherms. The linear form of the Langmuir model is shown in equation 4. The Freundlich isotherm provides an information encircling the heterogeneous surface [36]. The linearised form of Freundlich equation is shown in equation 7.

Figures 4a and 5 show the Langmuir and Freundlich plot for adsorption of Pb^{2+} onto CPCNC. The factors and the correlation coefficients (R^2) are indicated in Table 1. With reference to correlation coefficients, the experimental data were properly fitted into Langmuir and Freundlich having both R^2 value to be 1, thus R^2 value for both models are 1. The Langmuir isotherm proposes that adsorption was due to the formation of Pb^{2+} in contact with the surface of CPCNC while the Freundlich isotherm expresses a good surface heterogeneity of the active sites. The equilibrium parameter, RL, is a vital part of the Langmuir isotherm (Figure 4b) which is denoted as a separation factor and is a dimensionless constant [36]. The RL value indicates a favourable or unfavourable adsorption process. If RL>1, it unfavourable; if RL= 0, it is irreversible; if RL=1, it is linear; if 0<RL<1 it is favourable and feasible. In the adsorption of Pb^{2+} onto CPCNC, the values of RL ranged between 0.02 to 0.248 which is less 1, indicating that the adsorption was favourable.

The Freundlich adsorption plot for Pb^{2+} onto CPCNC showed that the constants n and K_f were derived from the plot of Lnqe against LnCe; n is 1 which is far lower than 10,

depicting that the adsorption was favourable. It also indicates a good affinity of the sorbent towards the uptake of the Pb^{2+} and 1/n indicates the function of the strength of the adsorption [36][33][38].

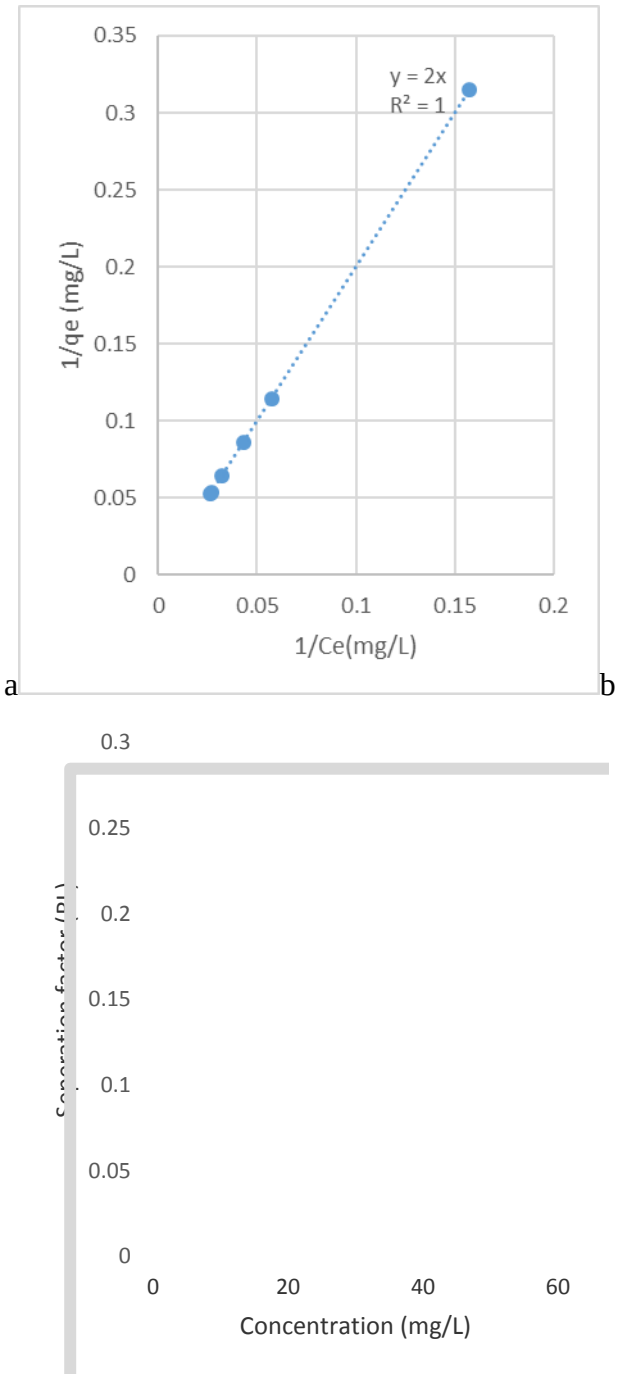

Figure 4a: (a) Langmuir isotherm (b) separation factor on the adsorption of Pb^{2+} onto CPCNC

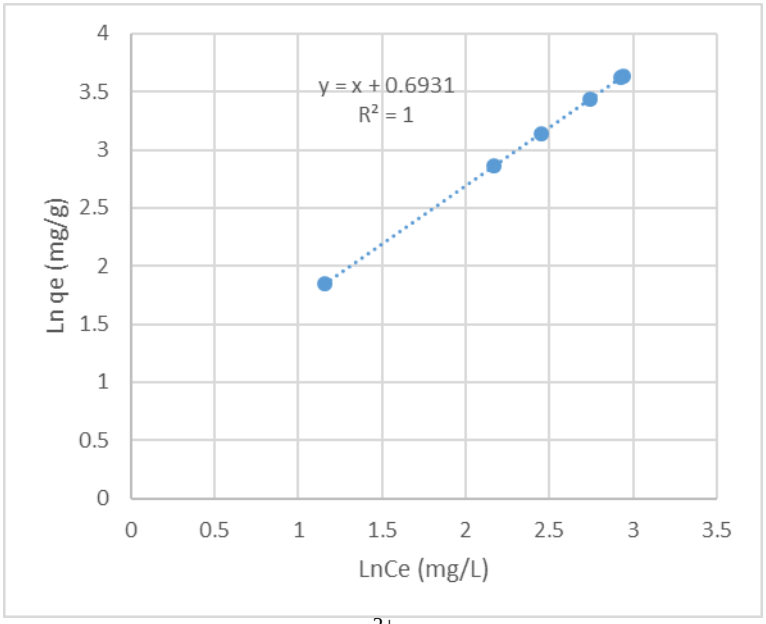

Figure 5: Freundlich model for adsorption of Pb^{2+} onto CPCNC

Table 1: Langmuir and Freundlich constant on adsorption of lead ion onto CPCNC

Isotherm models	Parameters	R^2
Freundlich	n= 1, 1/n = 1, K_f = 1.999,	1
Langmuir	Q_m= 0, b = 0.5, RL = 0.024-0.248	1

4. Conclusion

This research has effectively studied the preparation, characterisation and use of cellulose nanocrystal from cassava peel for the adsorption of Pb^{2+} from wastewater. The results indicate that the uptake of Pb^{2+} hinge on all the optimisation factors. The equilibrium adsorption data fitted well into both the Langmuir and Freundlich isotherm models, indicating a good adsorption process between the Pb^{2+} and the CPCNC. Hence, cellulose nanocrystal from cassava peel is a likely low-cost alternative nano-adsorbent material for the adsorption of Pb^{2+} from wastewater.

Acknowledgements

The authors sincerely appreciate the financial contributions of TETFUND (Nigeria), NRF/RISA (South Africa), Mr. Yunus Kippie of School of Pharmacy, University of the Western Cape, Cape Town, South Africa and the support of Professor Leslie Petrik for offering the laboratories and equipment for our research in the research laboratory of Environmental and Nano Science Group, University of the Western Cape.

References

[1] Onnby, L. (2013). Water treatment using cryogel-based adsorbents: Targeting environmental pollutants at low concentrations. Doctoral dissertation submitted to Lund University, Faculty of Engineering.

[2] Anazawa K., Kaid, Y., Shinomura, Y., Tomiyasu, T. and Sakamoto, H. (2004). Heavy – metal distribution in river waters and sediment around a Firefly Village, Shikoku, Japan. Application of multivariate analysis. *Analytical Science,* 20, 79 – 84.

[3] Suopajarvi, T. (2015). Functionalized nanocelluloses in wastewater treatment applications. Master's Thesis, Faculty of Technology, University of Oulu Graduate School, Finland. 1-76.

[4] Song, Y., Zhang, J. and Gan, W. (2010). Flocculation Properties and Antimicrobial Activities of Quaternised Celluloses Synthesized in NaOH/Urea Aqueous Solution. *Industrial and Engineering Chemistry Research,* 49(3), 1242-1246.

[5] Dada, A. O., Ojediran, J. O. and Abiodun, P.O. (2013). Sorption of Pb^{2+} from aqueous unto modified rice husk: Isotherm studies. *Advances in Physical Chemistry*, **2013:**1-6. Article ID 842425,http://dx.doi.org/10.1155/2013/842425.

[6] Inegbenebor, A. I., Inegbenebor, A. O. and Boyo, H. I. (2012). Comparison of the adsorptive capacity of raw materials in making activated carbon filter for purification of polluted water for drinking. *ARPN Journal of Science and Technology*, 2(9), 754-760.

[7] Hongjia, L., Yu G., Longhui, Z., and Xiong L. (2013). Morphological, crystalline, thermal and physicochemical properties of cellulose nanocrystals obtained from sweet potato residue. *Journal of Food Research International,* 50, 121-128.

[8] Peng, L. (2015). Adsorption behavior of heavy metal ions from aqueous medium on nanocellulose. Doctoral Thesis, Department of Engineering Sciences and Mathematics. Lulea University of Technology, Luleå, Sweden.

[9] Flauzino, N. W. P., Mariano, M., da Silva, I. S. V., Putaux, J. L., Otaguro, H., Pasquini,D. and Dufresne, A. (2016). Mechanical properties of natural rubber nanocomposites reinforced with high aspect ratio cellulose nanocrystals isolated from soy hulls. *Carbohydrate Polymers,* 153, 143-152.

[10] Ng, H. M., Sin, L. T., Tee, T. T., Bee, S. T., Hui, D., Low, C. Y. and Rahmat, A. R. (2015). Extraction of cellulose nanocrystals from plant sources for application as reinforcing agent in polymers. *Composites Part B: Engineering,* 75, 176–200.

[11] Aro, S. O., Aletor, V. A., Tewe, O. O. and Agbede, J. O. (2010). Nutritional potentials of cassava tuber wastes: A case study of a cassava starch processing factory in south-western Nigeria. *Livestock. Research for Rural Development,* 22 (11), 1-11.

[12] Tewe, O. O. (2004). The global cassava development strategy: cassava for livestock feed in Sub-Saharan Africa. IFAD and FAO.1-75.

[13] Lu, P. and Hsieh, Y. (2012). Preparation and characterization of cellulose nanocrystals from rice straw. *Carbohydrate Polymers,* 87, 564– 573.

[14] Rahimi, M. K. S., Brown, R. J., Tsuzuki, T. and Rainey, T. J. (2016). A comparison of cellulose nanocrystals and cellulose nanofibres extracted from bagasse using acid and ball milling methods. *Advances in Natural Sciences: Nanoscience and Nanotechnology*, 7, 1-9. http://dx.doi.org//:10.1088/2043-6262/7/3/035004

[15] Shaheen, T. I. and Emam, H. E. (2018). Sono-chemical synthesis of cellulose nanocrystals from wood sawdust using Acid hydrolysis. *International Journal of Biological Macromolecules*, 107, 1599-1606.

[16] Anuj, K., Yuvraj, S. N., Veena, C. and Nishi, K. B. (2014). Characterization of cellulose nanocrystals produced by acid-hydrolysis from sugarcane bagasse as agro-waste. *Journal of Materials Physics and Chemistry*, 2(1), 1-8.

[17] Naduparambath, S., Jinitha, T. V., Shaniba, V., Sreejith, M. P., Aparna, K. B, and Purushothaman, E. (2018). Isolation and characterisation of cellulose nanocrystals from sago seed shells. *Carbohydrate Polymers,* 180, 13–20.

[18] Azubuike, C. P., Rodríguez, H., Okhamafe, A. O. and Rogers, R. D. (2012). Physicochemical properties of maize cob cellulose powders reconstituted from ionic liquid solution. *Cellulose,* 19(2), 425–433.

[19] Seagal, L., Creely, J. J., Martin, A. E. and Conrad, C. M. (1959). An empirical method for estimating the degree of crystallinity of native cellulose using X-ray diffractometer. *Textile Research Journal*, 29, 786-794.

[20] Ho, Y. S. (2004). Pseudo-isotherms using a second order kinetic expression constant. *Adsorption,* 10, 151–158.

[21] Ahmad, M. A., Ahmad, N. and Bello, O. S. (2014). Modified durian seed as adsorbent for the removal of methyl red dye from aqueous solutions. *Applied Water Science,* 5(1), 407-423. doi:10.1007/s13201-014-0208-4

[22] Nascimento, D. M. D., Almeida, J. S., Vale, M. D. S., Leitão, R. C., Muniz, C. R., Figueirêdo, M. C. B. D. (2016). A comprehensive approach for obtaining cellulose nanocrystal from coconut fiber. Part I: Proposition of technological pathways. *Industrial Crops and Products,* 93, 66-75.

[23] Deepa, B., Abraham, E., Cordeiro, N., Mozetic, M., Mathew, A. P., Oksman, K. (2015). Utilization of various lignocellulosic biomass for the production of nanocellulose: A comparative study. *Cellulose,* 22(2), 1075-1090.

[24] Ilyas, R. A., Sapuan, S. M., Ishak, M. R. (2018). Isolation and characterization of nanocrystalline cellulose from sugar palm fibres (Arenga Pinnata). *Carbohydrate Polymers,* 181, 1038–1051.

[25] Morais, J. P. S., Rosa, M. F., Filho, M. M. S., Nascimento, L. D., Nascimento, D. M., Cassales, A. R. (2013). Extraction and characterization of nanocellulose structures from raw cotton linter. *Carbohydrate Polymers,* 91, 229-235.

[26] Thambiraj, S. and Ravi, S. D. (2017). Preparation and physicochemical characterization of cellulose nanocrystals from industrial waste cotton. *Journal of Applied Surface Science,* 412, 405–416.

[27] Klemm, D., Heublein, B., Fink, H. P. and Bohn, A. (2005). Cellulose: Fascinating Biopolymer and Sustainable Raw Material. *Angewandte Chemie International Edition,* 44(22), 3358–3393. http://dx.doi.org/10.1002/anie.200460587.

[28] Mohammad, M. A., Salleh, W.N. W., Jaafar, J., Ismail, A. F., Mutalib, M. A., Mohamad, A. B., Zaind, M. F. M., Awang, N. A. and Mohd Hir, Z. A. (2017). Physicochemical characterization of cellulose nanocrystal andnanoporous self-assembled CNC membrane derived from Ceibapentandra. *Carbohydrate Polymers*, 157, 1892-1902.

[29] Nurain, J., Ishak, A, and Dufresne, A. (2012). Extraction, preparation and characterization of cellulose fibres and nanocrystals from rice husk. *Industrial Crops and Products,* 37, 93-99.

[30] Buong, W. C., Syn, H. L., Nor, A. I., Yoon, Y. T. and Yuet, Y. L. (2017). Isolation and Characterisation of Cellulose Nanocrystals from Oil Palm Mesocarp Fiber. *Polymers*, 9, 1-11. http://dx.doi.org//: 10.3390.

[31] Widiarto, S., Yuwono, S. D., Rochliadi, A. and Arcana, I. M. (2017). Preparation and Characterisation of Cellulose and Nanocellulose from Agro-industrial Waste - Cassava Peel. *IOP Conference Series Material Science and Engineering,* 176, 012052 http://dx.doi.org//:10.1088/1757-899X/176/1/012052.

[32] Zain, N. F. M., Salma, M. Y. and Ishak, A. (2014). Preparation and Characterization of Cellulose and Nanocellulose from Pomelo (*Citrus grandis*) Albedo. *Journal of Nutrition and Food Science,* 5(1), 334. http://dx.doiorg//:10.4172/2155-9600.1000334.

[33] Bode-Aluko, C. A. (2017). Functionalisation of polymer nanofibres and track-etched membrane for removal of organic and inorganic pollutants from water. Ph.D. Thesis, University of the Western Cape, Cape Town, South Africa.

[34] Hugo, V., Lennart, B., Peng, L. and P. M. Aji, (2017). Nanocellulose-Based Materials for Water Purification. *Nanomaterials,* 7(3), 57. Doi: 10.3390/nano7030057.

[35] Liu, P., Sehaqu, I. H., Tingaut, P., Wichser, A., Oksman, K. and Mathew, A. P. (2014). Cellulose and chitin nanomaterials for capturing silver ions (Ag+) from water via

surface adsorption. *Cellulose,* 21, 449–61. http://dx.doi.org/10.1007/s10570-013-0139-5

[36] Dada, A. O., Adekola, F. A. and Odebunmi, E. O. (2015). A novel zerovalent manganese for removal of copper ions: synthesis, characterization and adsorption studies. *Applied Water Science,* http://dx.doi.org//: 10.1007/s13201-015-0360-5.

[37] Kumar, P. S. (2013). Adsorption of Lead (II) Ions from Simulated Wastewater Using Natural Waste: A Kinetic, Thermodynamic and Equilibrium Study. *Environmental Progress and Sustainable Energy,* 33 (1), 55-64. http://dx.doi.org// 10.1002/ep.

[38] Batmaz, R., Mohammed, N., Zaman, M., Minhas, G., Berry, R. M and Tam, K. C. (2014). Cellulose nanocrystals as promising adsorbents for the removal of cationic dyes. *Cellulose,* 21, 1655–65. http://dx.doi.org/10.1007/s10570-014-0168-8.